The relationship of winter season North Atlantic blocking frequencies to extreme cold or dry spells in the ERA-40

By TANIA BUEHLER[1,2], CHRISTOPH C. RAIBLE[1,2]* and THOMAS F. STOCKER[1,2],
[1]*Climate and Environmental Physics, Physics Institute, University of Bern, Sidlerstr. 5, CH-3012 Bern, Switzerland;*
[2]*Oeschger Centre for Climate Change Research, University of Bern, Sidlerstr. 5, CH-3012 Bern, Switzerland*

ABSTRACT

Atmospheric blocking is an important source of low-frequency variability. We apply a blocking detection and tracking method to ERA-40 data for the Atlantic-European region to assess linkages to extreme events, that is, cold and dry spells in the extended winter season (November-April). The method is feature-oriented, identifies 500-hPa geopotential height maxima, and connects them with a next-neighbourhood search in time. The analysis reveals a statistically significant decrease of number of blocking events over the period of ERA-40. Winters with an increased number of blocking events are associated with negative temperature anomalies over Central to Eastern Europe and dryer conditions, whereas Southern Europe experiences warmer and wetter conditions during such episodes. Using extreme value statistics we show evidence that cold spells, and to some extent dry spells, are strongly associated with extremes in blocking frequency. The number of cold spell days increases with the duration of blocking events indicating that cold spells need time to establish during blocking events, thus return periods of cold spells are longer than those for blocking events. This behaviour is not found for the relation of dry spells with blocking events. Still, blocking episodes have a higher occurrence of dry spells than climatology.

1. Introduction

One of the most prominent features of mid-latitude atmospheric variability is blocking. Blocking events are quasi-stationary anticyclones with an equivalent barotropic signature. Moreover, in the seminal study of Rex (1950) a blocking event is understood as a breakdown of the westerly flow, that is, the ambient westerly flow in the mid-latitudes is replaced locally with the easterlies. Temporally, blocking events are characterized as their persistence for several days (7 d and longer). These longer time scales have led to renewed interest during the last decades because of their potential to improve the predictability beyond classical numerical weather prediction.

In the North Atlantic, blocking events are often associated with a 'high-over-low situation' (a high located north of a low on a similar longitude) or sometimes with a particular large-scale weather type consisting of a high on the poleward side with upstream and downstream low pressure systems on the equatorward side (resulting in an Ω-shape of the isobars). Due to the persistent and quasi-stationary nature of blocking events, changes in their frequencies and duration could have a significant impact on monthly and even seasonal climate conditions, like temperature and precipitation (Fraedrich et al., 1993; Trigo et al., 2004).

Different concepts of the underlying dynamical processes generating blocking-like events are proposed in the literature. Egger (1978) suggested a non-linear interaction of orographically forced waves with slow moving free waves, whereas Charney and DeVore (1979) found that blocking phenomena are associated with multiple flow equilibria. Nakamura et al. (1997) suggested that the quasi-stationary Rossby wave train is important in the formation of blocking events over Europe. Pelly and Hoskins (2003) identified Rossby wave breaking of potential temperature on potential vorticity surfaces using the potential vorticity framework (Hoskins et al., 1985). These concepts led to a variety of different blocking indices and associated blocking climatologies. Some indices are based on the meridional geopotential height gradient (Lejenäs and Økland, 1983; Tibaldi and Molteni, 1990) and the detection of geopotential height maxima on the 500 hPa level (Sausen et al., 1995). More recently, indices

based on potential temperature on potential vorticity surfaces (Pelly and Hoskins, 2003; Tyrlis and Hoskins, 2008a,b) and vertically integrated potential vorticity (Schwierz et al., 2004) have been developed.

Current studies deduce blocking climatologies and investigate their characteristics and connections to the mean flow (Sinclair, 1996; Shabbar et al., 2001; Pelly and Hoskins, 2003; Barriopedro et al., 2006; Scherrer et al., 2006; Croci-Maspoli et al., 2007; Woollings et al., 2008). Barriopedro et al. (2006) and Croci-Maspoli et al. (2007) showed that blocking events in the North Atlantic region decrease in frequency and their life time is reduced for the reanalysis period 1958–2001. Note that this decrease is consistent with the observed positive trend in North Atlantic/Arctic Oscillation (NAO/AO) during this period as found by, for example, Thompson et al. (2000).

Besides the interaction of atmospheric blocking with the mean flow, atmospheric blocking events can lead to extreme weather events, as shown in, for example, Hoskins and Sardeshmukh (1985); Sinclair (1996); Black et al. (2004); Trigo et al. (2005) and Garcia-Herrera et al. (2007). Focusing on particular events, these case studies show that blocking can be related to severe droughts and heat waves like summer 2003, for example, Black et al. (2004) or the extremely cold conditions in the winter 1985–1986 in northwestern Europe (e.g. Hoskins and Sardeshmukh 1987). Takaya and Nakamura (2005b) investigated the blocking formation impacting the Siberian high and showed that regardless of the particular type of blocking formation cold air outbreaks at the northeastern slopes of the Tibetan Plateau are prominent. They further emphasize that the baroclinic structure of these events plays an important role in developing cold spells of the Siberian continent (Takaya and Nakamura, 2005a). More recently, Sillmann and Croci-Maspoli (2009) combine the blocking events, detected by the algorithm of Schwierz et al. (2004), with extreme monthly indices, such as the minimum of the minimum 2-m temperature as described by Frich et al. (1996, 2002). Based on a correlation analysis they found that the connection between blocking events and cold winter temperature is robust also in a future climate state.

The purpose of this study is to utilize extreme value theory in order to investigate the relation among different extreme events, like extremely long blocking events, cold and dry spells. To assess the behaviour of blocking events we developed an event-based method, which combines elements from existing methods such as geopotential height gradient (Tibaldi and Molteni, 1990), the geopotential height maxima (Sausen et al., 1995; Sinclair, 1996) and a subsequent tracking (Sinclair, 1996; Schwierz et al., 2004). To show the method's ability we test the mean behaviour against another technique of Scherrer et al. (2006), who extend the method of Tibaldi and Molteni (1990) to two dimensions. To investigate the impacts to other extremes for the North Atlantic European region cold and dry spells are defined. The overall aim is to assess the 'on average' dynamical linkage between extreme

atmospheric blocking and dry and cold spell during the extended winter season.

The outline of the study is as follows: In Section 2 the data and the technique of Scherrer et al. (2006) are briefly introduced and the event-based method is presented in more detail. Then, the event-based method is compared to Scherrer et al. (2006) with respect to the mean in Section 3. Section 4 focuses on the extreme value statistics and the relation between extreme blocking events and cold and dry spells. Finally, the results are discussed and conclusions are presented (Section 5).

2. Data and analysis techniques

The study is based on the ERA-40 data set provided by the European Center for Medium-Range Weather Forecasts (ECMWF). We use the 500-hPa geopotential height, the 2-m temperature, and the total precipitation from 1957 to 2002 on a regular grid of $2.5° \times 2.5°$ and 6-hr time resolution. The focus is set to the extended winter season November to April (NDJFMA).

To identify blocking events, two methods are used. As there is no strict definition of blocking events the identification of such events can be based on several indicators. An already existing method (hereafter S06 method) expanded the latitudinal-based method of Tibaldi and Molteni (1990) to a 2-D index (Scherrer et al., 2006). Meridional geopotential height gradients south ($\nabla_s Z$) and north ($\nabla_n Z$) are calculated for each grid point in the region 35°N to 75°N with $\Delta\phi = 2.5°$ intervals as follows:

$$\nabla_s Z(\phi) = \frac{Z(\phi) - Z(\phi - \Delta\phi)}{\Delta\phi}, \tag{1}$$

$$\nabla_n Z(\phi) = \frac{Z(\phi + \Delta\phi) - Z(\phi)}{\Delta\phi}. \tag{2}$$

A grid point is treated as a blocked situation, if the two following gradient criteria are fulfilled:

$$\nabla_s Z(\phi) > 0 \text{ and } \nabla_n Z(\phi) < -10 \text{ gpm/deg lat}. \tag{3}$$

As blocking is persistent in time, an additional duration criterion of a minimum of 3 d is added, which considers the number of consecutive blocked situations at one grid point. The duration criterion additionally includes a stationarity criterion, because the consecutive grid points have all the same longitude and latitude. Note that the spatial extent (roughly a few thousand kilometres in diameter) of a blocking event and the life cycle are not included in this method.

To include additional characteristics of blocking events, like the spatial extent and the life cycle the so-called Lagrangian blocking method (LB method) is developed. Note that other methods, for example, the methods by Sinclair (1996) and by Schwierz et al. (2004) already tackle shortcomings of the S06 method. The LB method is based on a cyclonic detection and tracking method originally invented for mid-latitude cyclones (Blender et al., 1997) and is to some extent similar to the method

of Sinclair (1996). For this study the algorithm includes some new parameters to detect and refine the blocking feature. The underlying algorithm consists of two steps: detection and tracking. First, local maxima and the mean geopotential height gradient (∇z_{500}) around the local maximum are identified in the 500-hPa geopotential height field. The ∇z_{500} is the arithmetic average of the calculated gradients between the geopotential height maximum and its neighbour grid points within an area of $\simeq 1000$ km radius around the geopotential height maximum:

$$\nabla_s z_{500} = \sum_{i=-m}^{m} \sum_{j=-n}^{n} \frac{Z_0 - Z(i, j)}{\sqrt{(i \Delta x)^2 + (j \Delta y)^2}}, \tag{4}$$

where Z_0 is the identified maximum geopotential height, $2m+1$ and $2n+1$ the number of grid points in longitude and latitude, respectively. Δx and Δy are the increments in longitude and latitude, that is, $\Delta y = 278$ km and Δx depends on the latitude of Z_0 (at 60°N it is 140 km, at 45°N it is 197 km). Thus, in contrast to the S06 method the ∇z_{500} criterion takes also the gradients in zonal direction into account. The ∇z_{500} has to exceed a threshold, called the minimum geopotential height gradient ($\nabla z_{500} = 40$ gpm $(1000$ km$)^{-1}$). Second, the tracking part uses the information of the consecutive geopotential height field. Two centres belong together, if a geopotential maximum within a radius of $\simeq 1000$ km, which corresponds to the Rossby deformation radius, is found in the geopotential height field 6 hr before. Two other criteria are used to reduce artificial maxima: One parameter determines the minimum life time of a blocking event, which is set to 3 d, and the second condition is that the ∇z_{500} exceeds a threshold of $\nabla z_{500} = 55$ gpm $(1000$ km$)^{-1}$ at least once in the life time of the anticyclone track. In addition, areas of altitude higher than 1000 m are excluded by the algorithm to guarantee that the Greenland anticyclones are excluded as they are not able to efficiently block the westerly flow due to their far north position. Note that without this criterion the LB method already removes most of the rather weak Greenland anticyclones.

The LB method is sensitive to certain parameters. The most sensitive parameters are the minimum and maximum geopotential height gradients. To adjust those, the mean blocking frequency (similar to Fig. 1a) is estimated with varying values for both thresholds between 20 and 60 gpm $(1000$ km$)^{-1}$ (not shown). The blocking frequency, the regional blocking distribution and the number of split-up blocking events are considered to adjust the thresholds. Split-up blockings are those which precede or immediately follow (maximum time range of 1 d) another blocking and in its neighbourhood (maximum distance $\simeq 1000$ km). In general, the more restrictive the thresholds are, the fewer blockings are found and the blocking frequency decreases. Spatially, a value under 40 gpm $(1000$ km$)^{-1}$ leads to unrealistic blocking frequencies south of 40°N. Thus, the threshold for the minimum geopotential height gradient is set to 40 gpm $(1000$ km$)^{-1}$ to guarantee the absence of blocking frequen-

cies south of 40°N. The optimum threshold between 40 and 60 gpm $(1000$ km$)^{-1}$ for the maximum geopotential height gradient is 55 gpm $(1000$ km$)^{-1}$ with respect to a desired low number of split-up blockings and a reasonable total number of detected blockings that is high enough to do statistics.

To illustrate the ability of the LB method we show a case study from the 2 to 8 December 1962 for the North Atlantic European region (Fig. 2). The method identified an Ω-shape blocking event over the British Isles, which was rather stationary over the first 3–4 d. In its lysis phase the general weakening of the blocking went along with a slight displacement from the British Isles to the south. This is in good agreement with the results received from the S06 method for the same case study. The main area of blocked grid points was found at the same location as for the detected blocking area of the LB method. The area of the blocked grid points shifted also to the south during the blocking life cycle. The S06 method additionally detected a small area of blocked grid points west to Greenland, which was shifted 20° to the south during the blocking life cycle.

3. Blocking events in winter

To introduce the LB method we first compare it with the S06 method with respect to the blocking frequency distribution (Fig. 1). Straightforward comparison should not be made between Figs. 1a and b, because the S06 method shows the grid point based blocking frequency whereas the LB method is designed to count the centre blocking frequency. Note that the unit of blocking frequency is the ratio in percentage per $(1000$ km$)^2$. As one grid point in a regular grid of 2.5° × 2.5° represents less than $(1000$ km$)^2$ (e.g. $\simeq 275$ km × 275 km near the equator and $\simeq 6$ km × 275 km near the poles), the blocking frequency can exceed 100%. To give an example, the ERA-40 data set used in this study includes 32 624 time steps. Thus a blocking frequency of 180% means that 58 723 time steps are blocked within an area of $(1000$ km$)^2$. For a grid point near the equator (represents an area of $\simeq 275$ km × 275 km) this means 4441 time steps out of 32 642 are blocked.

The major blocking event centres are identified over Greenland, over England and Norway and over Russia based on the S06 method. The maximum over Greenland identified by the S06 method is related to Greenland anticyclones (Fig. 1b). As these anticyclones are located north of the main westerly flow, they have only a weak ability to block the westerly flow and have been excluded from our blocking statistics. The centre of high blocking frequency in the North Atlantic is located more westwards in the LB method than in the S06 method. Over Russia the LB method identifies another maxima, whereas this is less clear for the S06 method. The strict ∇z_{500} criteria of the LB method suppress the unrealistic blocking events south of 40°N making the LB method superior to the S06 method, as it only extracts those anticyclones which have the ability to block the westerly flow. Moreover, the pattern in Fig. 1a is similar to other methods,

Fig. 1. Mean blocking frequency in the North Atlantic in the winter (NDJFMA) from 1957 to 2002 (ERA-40 data set) using the (a) the LB method and (b) S06 method. The unit of blocking frequency is the ratio in percentage per $(1000\,\mathrm{km})^2$. As on grid point in a regular grid of $2.5° \times 2.5°$ represents less than $(1000\,\mathrm{km})^2$ (e.g. $\simeq 275\,\mathrm{km} \times 275\,\mathrm{km}$ near the equator and $\simeq 6\,\mathrm{km} \times 275\,\mathrm{km}$ near the poles), the blocking frequency can exceed 100%. To give an example, the ERA-40 data set used in this study includes 32 624 time steps. Thus a blocking frequency of 180% means that 58 723 time steps are blocked within an area of $(1000\,\mathrm{km})^2$. For a grid point near the equator (represents an area of $\simeq 275\,\mathrm{km} \times 275\,\mathrm{km}$) this means 4441 time steps out of 32 642 are blocked. Note that the LB method only counts the centre of the blocking, whereas the S06 method counts every blocked grid point in the area of $(1000\,\mathrm{km})^2$. The outline in (a) illustrates the region $40°\mathrm{W}–40°\mathrm{E}$ and $35°\mathrm{N}–85°\mathrm{N}$ used to define an index of blocked situation (see text for details).
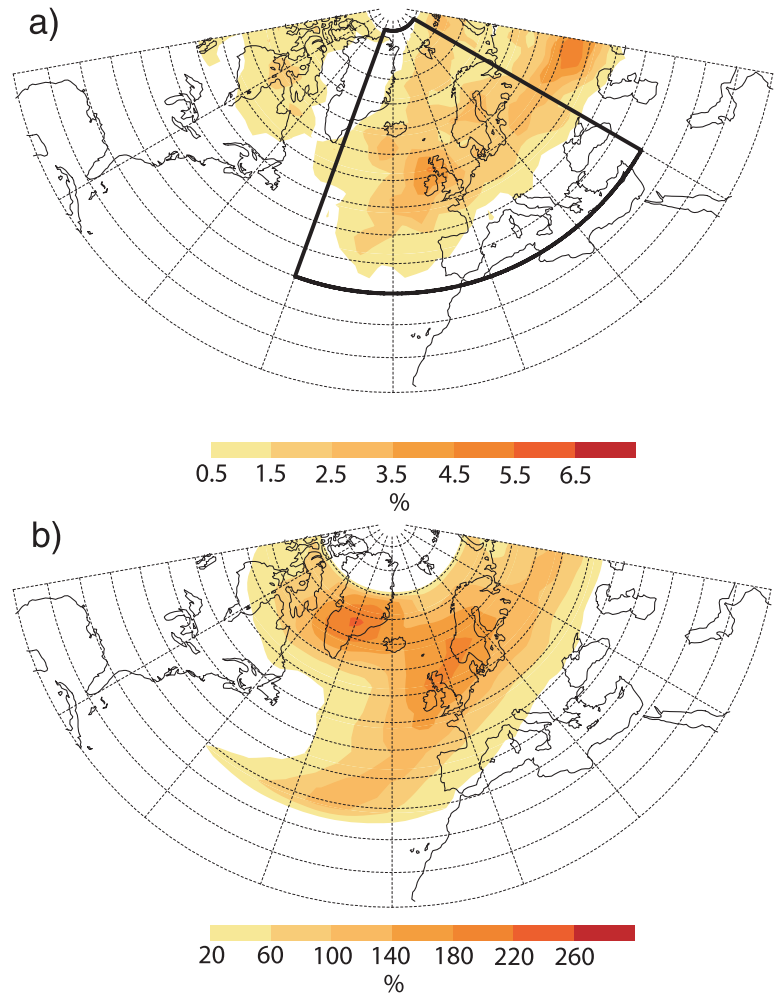
for example, Schwierz et al. (2004). Therefore, we exclusively use the LB method in the following.

Besides the general spatial distribution of blocking events we investigate the life time of blocking events and their time behaviour for the region $40°\mathrm{W}–40°\mathrm{E}$ and $35°\mathrm{N}–85°\mathrm{N}$ using the LB method. The number of blocking events decreases strongly with their duration (Fig. 3a). Note that the decrease is not exponential as the Chi-squared and Kolmogorov–Smirnov tests show. The average life time is 19.4 time steps (4.85 d). Notable are deviations from the monotonic decrease suggesting that blocking events of 16–17 ($\simeq 4$ d), 20–21 ($\simeq 5$ d) and 25–27 ($\simeq 8$–9 d) time steps are more frequent. This is in good agreement with the findings of Sausen et al. (1995). To investigate the interannual variability an index is defined using the number of blocked half-days per season in the region $40°\mathrm{W}–40°\mathrm{E}$ and $35°\mathrm{N}–85°\mathrm{N}$ (in the following $B_{1/2}$ index; Fig. 3b). In principle, such an index should use the maximum temporal resolution available (here 6 hrs) to include the full life cycle of blocking events. For the sake of future investigations of climate model output, which is often saved 12 hourly, we introduce the index of blocked half-

days. Note that the region used for the $B_{1/2}$ index excludes the maximum over Russia, to focus on those blocking events that lead to the breakdown of westerlies over Europe. The $B_{1/2}$ index decreases significantly with time (98% confidence interval). This negative trend is insensitive to the selected minimum life time of a blocking event as illustrated by Fig. 3c. The mean number of blocked half-days is 105 per season with a standard deviation of 30, if the minimum duration is set to be 3 d (Fig. 3b). Nearly all years with extreme high or low blocking events as detected by the $B_{1/2}$ index based on blocking events with at least 3 d durations are also identified by the $B_{1/2}$ index with an 8-d criterion (the upper 10%). The negative trend of the $B_{1/2}$ index is consistent with earlier studies (e.g. Barriopedro et al., 2006) and agrees with the trend observed for the NAO/AO towards its positive phase for the last two decades of the 20th century (e.g. Thompson et al., 2000), that is, towards a more zonal (i.e. non-blocked) flow regime.

As shown in Fig. 1 there is a maximum in blocking frequency near the British Isles, which impacts mean temperature and precipitation over Europe (e.g. Fraedrich et al., 1993; Trigo et al.,
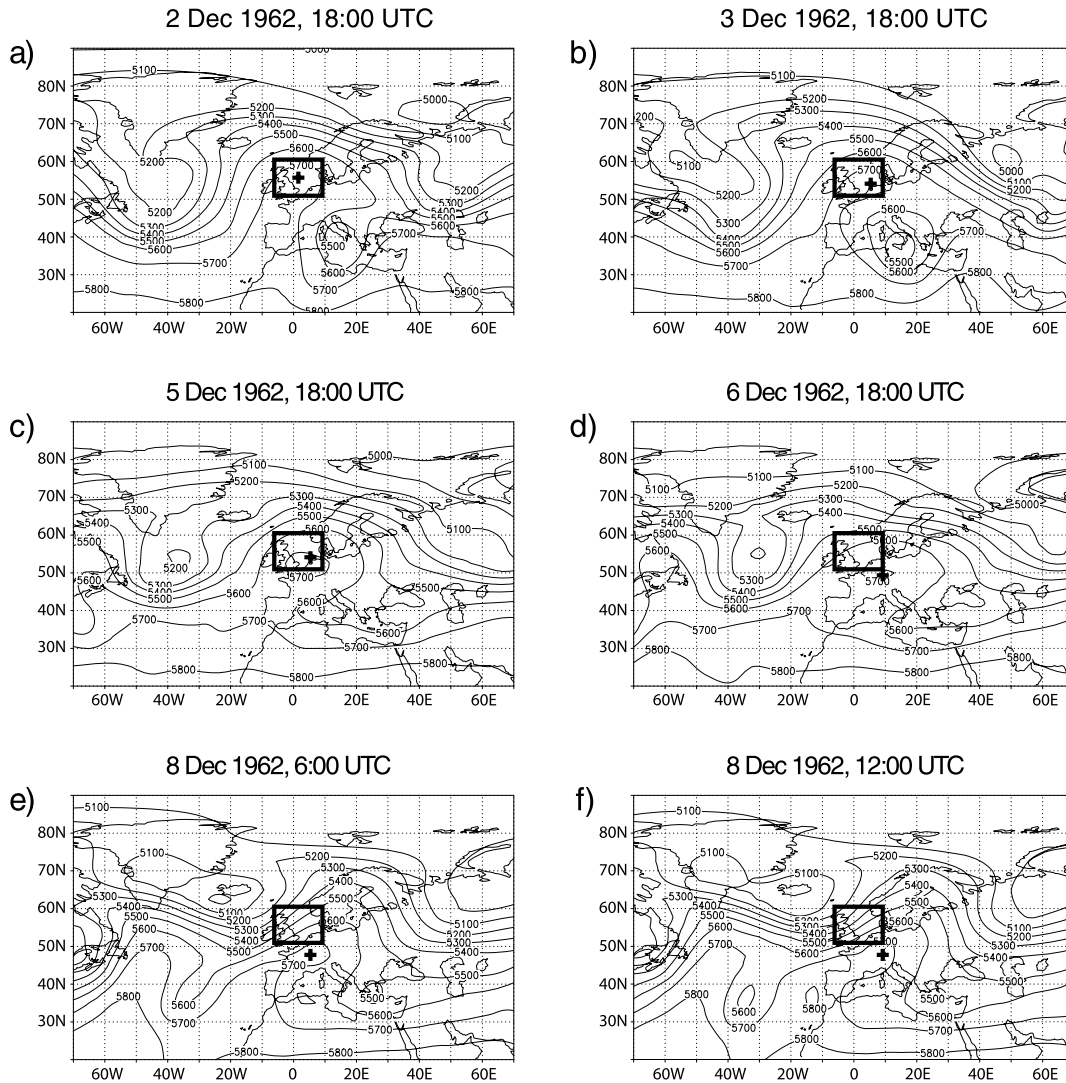
2 Dec 1962, 18:00 UTC

3 Dec 1962, 18:00 UTC

5 Dec 1962, 18:00 UTC

6 Dec 1962, 18:00 UTC

8 Dec 1962, 6:00 UTC

8 Dec 1962, 12:00 UTC

Fig. 2. 500-hPa geopotential height field (in gpm) for (a) 2 December 1962 18 UTC, (b) 3 December 1962 18 UTC, (c) 5 December 1962 18 UTC, (d) 6 December 1962 18 UTC, (e) 8 December 1962 6 UTC and (f) 8 December 1962 12 UTC. The cross shows the blocking centre and the rectangle shows the area resembling the dimension of the blocking. The rectangle represents the area used to deduce the mean geopotential height gradient (∇z_{500}). The contour interval is 100 gpm. The rectangle is held on the same place as in the first time step to better show the movement of the blocking centre.

2004). We use this known connection to further test our LB method. Therefore, we applied a composite analysis using the $B_{1/2}$ index. If the index of a particular winter season exceeds the mean plus (minus) one standard deviation (see Fig. 3b), the seasonal-mean field of the investigated variable (geopotential height, temperature or precipitation) is used to form the typical pattern of the variable during a phase of high (low) blocking frequency. In addition, a student *t*-test is performed using the 90% confidence level (applying the Mann-Whitney test slightly decreases the area of significance, not shown). First, the robustness of the difference between the typical pattern during a phase of high or low blocking frequency index is tested against the mean pattern of the total time series. This analysis shows that the two

patterns—either with high blocking frequency or low blocking frequency—are linear for all variables (not shown). Thus to show the effect of blocking we simply display the difference patterns between high and low blocking frequency.

To confirm that the LB method and the index are suitable for detecting blocking events near the British Isles, the composite analysis is applied to the seasonal-mean 500-hPa geopotential height. As expected the geopotential height difference shows a 'high-over-low situation' (Fig. 4a) for the North Atlantic in winter, resembling the findings of Trigo et al. (2004). Figure 4b shows seasonal-mean 2-m temperature differences between high and low $B_{1/2}$ index situations in winter. The typical temperature anomaly pattern related to high $B_{1/2}$ index shows a warming
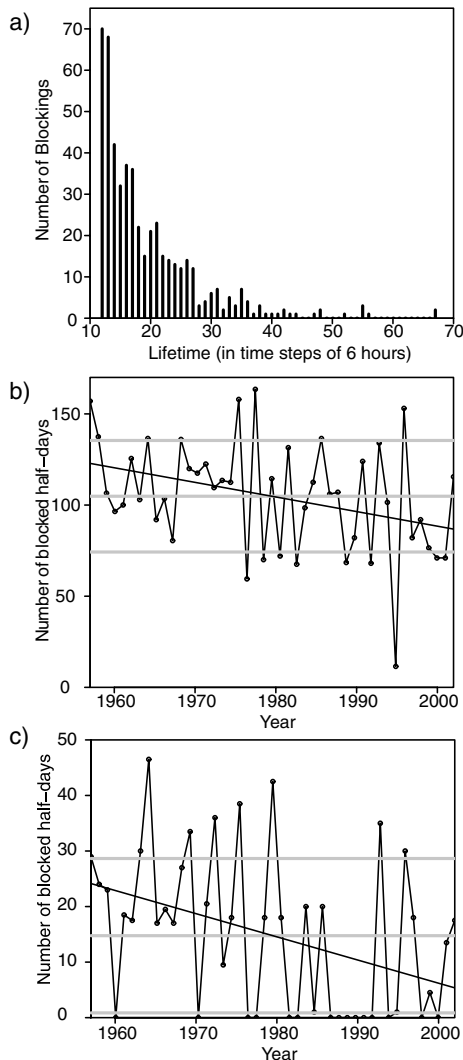
Fig. 3. (a) Life time of blocking events in the North Atlantic over the whole ERA-40 winter periods, (b) number of blocked half-days per season with trend line (significant at the 98% level) in the North Atlantic over the whole ERA-40 winter periods for blocking events with a duration of at least 3 d and (c) the same as (b) but or blocking events with a duration of at least 8 d (upper 10%). Grey lines in (b) and (c) indicate plus/minus one standard deviation and the mean.

Fig. 4. Difference between high and low $B_{1/2}$ index in the North Atlantic over the entire ERA-40 winter periods for the (a) seasonal-mean 500-hPa geopotential height ($m^2 s^{-2}$), (b) seasonal-mean 2-m temperature (K), and (c) precipitation (number of days >1 mm per day precipitation during the season). The thick black lines mark the significant differences on a 10% significance level.

(significant) over Greenland ($\simeq 2.5$ K) and south of Iceland ($\simeq 0.75$ K). Over the Eurasian continent it is colder (significant) during seasons with high $B_{1/2}$ index. For a low $B_{1/2}$ index the behaviour is the opposite.

Besides temperature, the impact on precipitation is of interest. Therefore, we compare the number of days per season with more precipitation than 1 mm per day of seasons with high and low blocking index situations (Fig. 4c). The number of days with more than 1 mm per day is significantly lower around the British Isles and Northern Europe in winter during a phase of high $B_{1/2}$ index compared to situations with a low $B_{1/2}$ index. A significant wetter region is found over Southern Europe.
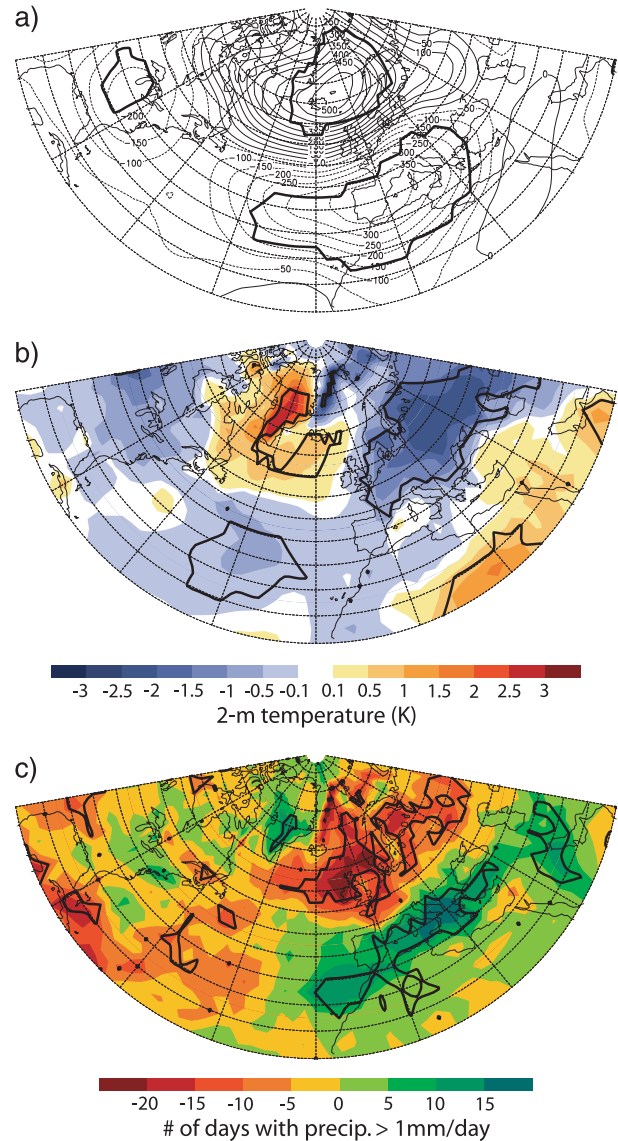
In summary the method shows that it is able to identify blocking features and their relationship to the seasonal-mean weather conditions for a given winter.

4. Extreme blocking events, cold and dry spells

In the following, we address the behaviour and the connections between different extreme events applying extreme-value statistics (see appendix) to the blocking life time, temperature and
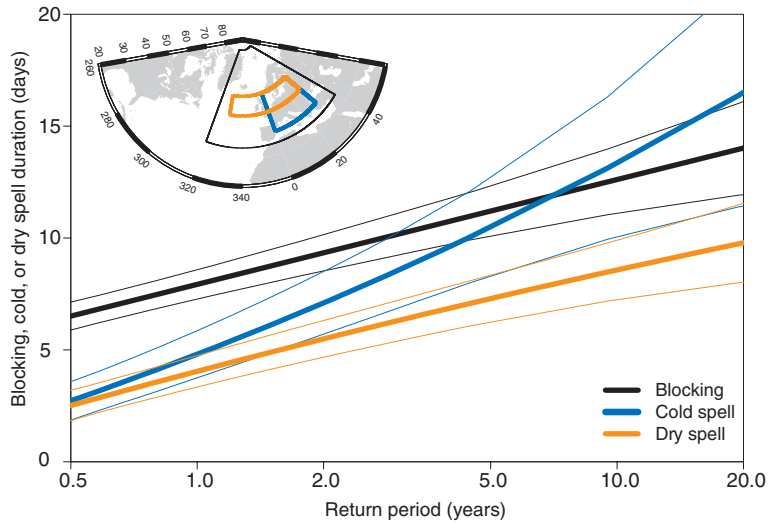
Fig. 5. Return periods for blocking events, cold and dry spells in the North Atlantic over 45 ERA-40 winters. The thresholds of the cold and dry spells are the 10th percentile values of the spatially averaged 2-m temperature anomaly over the area 0–30°E and 40-60°N and of the mean precipitation amount over the area 30°W–30°E and 50–60°N, respectively. The thin lines denote the 95% confidence interval (see appendix).

precipitation. The maximum life time of a blocking event, a cold and a dry spell per season forms the extreme-value data set. Thus, the assumption is that the data sets converge to a generalized extreme value (GEV) distribution (see the appendix), from which we determine return periods and the corresponding 95% confidence intervals (Fig. 5). A return period is the expected average time interval between to independent extreme events of the same characteristics, for example, life time.

The longest blocking life time per season in the area shown in Fig. 1a is selected as an extreme value. As the ERA-40 winter data set consists of 45 seasons the corresponding extreme-value data set contains 45 values of blocking life times. Figure 4b shows that blocking is related to a cooling over Europe. To investigate the relationship between the extreme blocking length and the duration of a so-called cold spell over Europe we compare their return periods. A cold spell is defined as follows: from the daily mean 2-m temperature fields the daily climatology over the whole ERA-40 winter period for the corresponding calendar day is removed. Then, an area average over 0–30°E and 40–60°N is calculated and denoted as the spatially averaged anomaly. If such an anomaly is below a certain threshold, the day is treated as a 'cold spell situation'. Consecutive spatially averaged anomalies, which are lower than the threshold, form a cold spell event. The cold spells thus identified over Europe were counted for a given winter season and the longest cold spell in the particular winter was registered for the extreme value data set. To test the sensitivity of the threshold, three different values are chosen, the 10th, 15th and 20th percentile (-3.0 K, -2.4 K and -1.9 K) of the spatially averaged anomaly. The threshold should be as low as possible, but there has to be at least one cold spell per season. The 10th percentile is used as it fulfills these criteria. Note that this relative definition was selected because of the extended winter season used in this study. In general, the return periods get shorter with a less extreme threshold (not shown). However,

the slope of the return periods does not change for less restrictive thresholds.

As evident in Fig. 5, the dependence of return period on event duration differs substantially between cold spells and blocking flow configurations. An agreement is found around the blocking and cold spell lengths of about 10 d, which have a return period of 5 yr. Note that using a less restrictive threshold leads to a shift of intersection with the blocking return periods to 5–7 d (not shown). The different slopes of the return periods of blocking and cold spell suggest that a rare cold spell event shows a tendency of being more persistent than an according rare blocking event with a comparably long return period, whereas for more frequent events with return periods around 2 yr or less the blocking event tends to be more persistent than the according cold spell event.

To understand the discrepancy between the return period of the blocking events and the cold spells, the conditional distribution between blocking events and cold spells is estimated. For each blocked situation the spatially averaged temperature anomaly is examined whether it is a cold spell situation or not. Figure 6a shows the fraction of those events that concur with cold spells among the blocking events as a function of their duration. If the blocking events and the cold spells are consistent, the ratio would be 1. The conditional distribution shows an increase of the cold spell ratio with increasing blocking duration. This means that the development of a cold spell takes time during blocking events explaining the different slopes of return periods in Fig. 5. To further confirm this relation the individual temperature life cycles of blockings are investigated. For 5-day blocking events a substantial decrease in temperature is found at the end of the life cycle (not shown). Longer blocking events, for example, 11–13 d, show no explicit trend; temperature tends to remain extremely low over the entire life cycle (not shown).

The connection of blocking and mean precipitation suggests that the area over the British Isles is dryer than normal during a
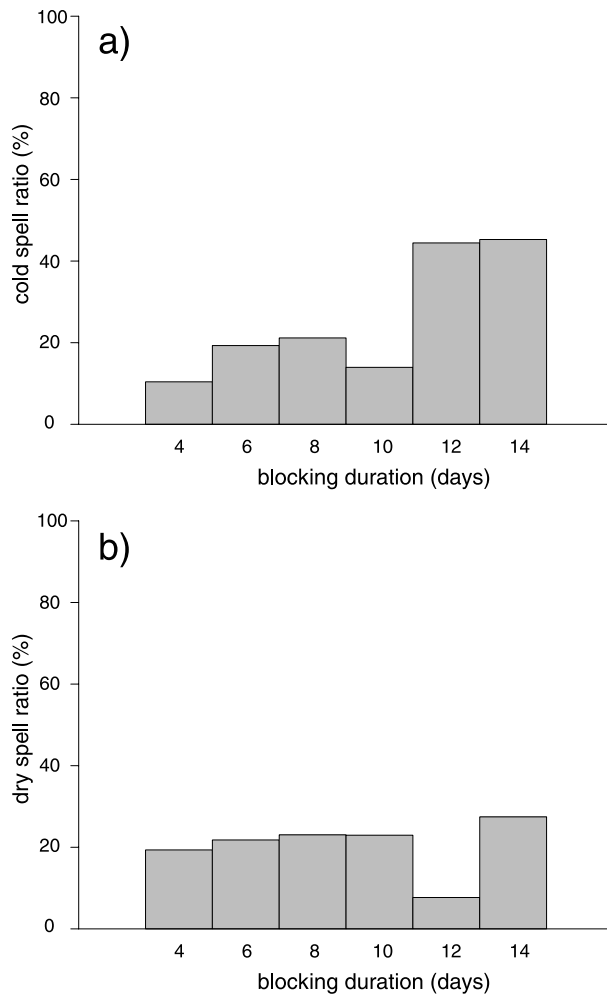
Fig. 6. Conditional distribution of (a) cold spells and (b) dry spells given the length of the blocking event. The thresholds of the cold and dry spells are the 10th percentile values of the spatially averaged 2-m temperature anomaly over the area 0–30°E and 40–60°N and of the mean precipitation amount over the area 30°W–30°E and 50–60°N, respectively. The bin width of the *x*-axis is 2 d; label is its centre.

phase of high $B_{1/2}$ index in the North Atlantic (see Fig. 4c). To investigate the linkage between extreme blocking and extremes in precipitation a dry spell is defined by an extremely low mean precipitation amount over the area from 30°W to 30°E and from 50°N to 60°N and a life time of at least 1 d. Note that the area of dry spells deviates from the area of cold spells as the mean impact of blocking events is different (Fig. 4c). Return periods for dry spells with different threshold values for the mean precipitation amount over the above-mentioned area are calculated. Similar to the definition of cold spells the threshold is set to the 10th (15th, 20th) percentile value of the daily precipitation amount corresponding to 1.0 (1.2, 1.4) mm per day, respectively. The higher the threshold, the shorter is the return period for a dry spell of specified length.

North Atlantic blocking events are compared with dry spells (see Fig. 5) in the winter season. With increasing return period the duration of a blocking or dry spell event gets longer at a comparable rate. Independent of the given return period a dry spell event tends to be less persistent than the according blocking event. This suggests that only some of the blocking events are accompanied by dry spell situations.

This discrepancy is again investigated by estimating the conditional distribution of the number of dry spell days during a blocking event. If the return period curves of both are similar, one would expect that most of the blocking days would be dry spell days at the same time. In our case the dry spells with a certain length are less frequent than the blocking events at the same length. The conditional distribution shows that the dry spell ratio is constant (roughly around 20%; Fig. 6b). This seems consistent with the similar slopes of the return periods of blocking events and dry spells. Note that a higher threshold for the dry spells leads to an increase of the constant dry spell ratio; the shape of the conditional distribution does not change (not shown). In the return level plot this would be seen as an increase in persistence for the dry spells. Nevertheless, the number of dry spell days is systematically increased by a factor of two during blocking events compared with the climatological background of 10% of the time.

5. Conclusions

This study investigates the connection of blocking events with extremes in cold and dry spells. For this purpose we have introduced a blocking detection and tracking method (LB method) which is to some extent similar to the method of Sinclair (1996), but differs substantially from the conventional detection methods by Lejenäs and Økland (1983); Tibaldi and Molteni (1990); Sausen et al. (1995); Pelly and Hoskins (2003) and Schwierz et al. (2004). Our method is based on a mid-latitude cyclone detection and tracking method (Blender et al., 1997), but modified for identification of blocking events. We allow our method to include part of the synoptic time scale (blocking duration greater than 3 d) to get more robust statistics. Note, however, that this choice does not affect any of the conclusions as confirmed through the same analysis (as mentioned above) but with a greater threshold for event duration. Both the S06 method and ours can identify the primary region of blocking around the British Isles, while unrealistic 'blocks' as identified south of 40 °N with the S06 method have been excluded with our method. This is in agreement with other methods, for example, the method by Schwierz et al. (2004) which identifies the major maximum of blocking events over the British Isles and no blocking events south of 40 °N. Moreover, unlike the S06 method, our method is feature-oriented but not grid-point based, which facilitates the investigation of blocking as a large-scale feature on, for example, extremes.

To further test the ability of the LB method the well-known relations to mean temperature and precipitation (Fraedrich et al., 1993; Trigo et al., 2004) are investigated. Clearly, increased blocking events in the North Atlantic detected by the LB method exhibit a cooling over Europe and a warming over Greenland and Iceland. The southern part of Europe is wet and the northern North Atlantic is dry during high $B_{1/2}$ index, resembling the findings by Fraedrich et al. (1993), Trigo et al. (2004) and thus giving further confidence in the method.

Besides the mean behaviour extreme blocking events and their implications are the major foci of this study. We defined cold spell days over a certain area by anomalies from the seasonal mean falling below the 10th percentile. Similar dry spell days are days over an area with a precipitation amount exceeding its 10th percentile. Both definitions deviate from the usual approach (Frich et al., 2002), for example, frost days, because of the extended season used. The relative measure for temperature, however, guarantees that all months are equally included in the analysis (a definition by e.g. frost days would focus only on December–February). These definitions are used to estimate return periods for blocking events, cold and dry spells. Return periods of blocking events compared with either return periods of cold or dry spells show no one-to-one correspondence. Blocking events of a specific length are more frequent than cold spells with the same life time. The analysis shows that the part of cold spell situations during a blocking event is more reduced for blocking events with shorter life times. This means that cold spells need time to develop during a blocking as shown by the conditional distribution and individual temperature life cycles. A rough estimate of the time lag could be deduced from the conditional distributions resulting in a lag of approximately 4–6 d. This interpretation agrees with finding from Nakamura and Fukamachi (2004), Takaya and Nakamura (2005b) and Takaya and Nakamura (2005a) who showed that blocking could induce anomalous surface winds which yields anomalous cold advection of up to approximately 1 °C per day. This suggests that it would take roughly 3 d to lower the temperatures over Europe. The development of a downstream (to the blocking) cyclonic anomaly due to southeastward emanation of Rossby wave activity could add another day to the time lag.

Return periods for dry spells of a specified length in the North Atlantic are generally longer than the return period of a blocking of the same length. In contrast to the cold spells the ratio of dry spells is independent from the duration of the blocking, but significantly increased compared with the climatological mean. Thus, extremes in blocking events are connected to both cold spells and dry spells in winter.

We have presented for the first time a comprehensive climatology-based overview of winter connections between extreme blocking events and other extreme events like cold and dry spells, which were suggested by case studies, for example, Hoskins and Sardeshmukh (1985); Black et al. (2004); Trigo et al. (2005) and Garcia-Herrera et al. (2007). Numerical weather prediction using ensemble prediction systems continuously improve their forecasts, among other things, by a better treatment of atmospheric blocking (e.g. O'Kane and Frederiksen, 2008). Thus, such connections give a first hint of how the predictability of extreme events, such as cold and dry spells in winter could be further improved.

6. Acknowledgments

7. Appendix

Extreme values are unusually larger than the rest of the data values. There are different ways to separate extreme values from the complete data. A common one is to pick out the maximum of a period of m-values. This is used here. A period can be associated with, for example, a winter season (NDJFMA), where the m-values are a list of, for example, the life times of the blocking events in this particular winter. If there are n winter seasons with each a list of m-values, the extreme value set consists of n values. This extreme value data set follows a generalized extreme value distribution (GEV) with a probability density function (Wilks, 2006) given by

$$f(x) = \frac{1}{\beta}\left[1 + \frac{\kappa(x - \zeta)}{\beta}\right]^{1 - \frac{1}{\kappa}} \exp\left\{-\left[1 + \frac{\kappa(x - \zeta)}{\beta}\right]^{-\frac{1}{\kappa}}\right\},$$
$$1 + \frac{\kappa(x - \zeta)}{\beta} > 0. \qquad (A1)$$

The cumulative density function of the GEV is

$$F(x) = \exp\left\{-\left[1 + \frac{\kappa(x - \zeta)}{\beta}\right]^{-\frac{1}{\kappa}}\right\}. \qquad (A2)$$

The parameter ζ denotes the location or shift parameter, β the scale parameter and κ the shape parameter. The m-values have to be independent and must come from the same distribution. This condition may not be fulfilled, because of an annual cycle. For that the data are divided into extended seasons.

A quantile can take an arbitrary value on the axis of abscissae of the cumulative probability density function $F(x)$. For a specified quantile x_p the following equation holds $F(x_p) = p$, where p denotes a probability between 0 and 1. Taking the inverse of this equation leads to the quantile function (for the GEV),

$$x_p = F^{-1}(p) = \zeta + \frac{\beta}{\kappa}[-ln(p)]^{-\kappa} - 1. \qquad (A3)$$

A return period is the expected average time interval between two independent extreme events of the same characteristics. For example, an event has a return period of 5 yr. Then the probability of appearance of an event at least once within 5 yr is 100%. The return period t of a GEV is calculated as follows:

$$t = \frac{1}{1 - F(x_t)}, \tag{A4}$$

x_t denotes the associated return level to the return period t, and $F(x)$ is the cumulative distribution function of the GEV. The equation for the return level x_t is given by

$$x_t = \zeta + \beta(y_t^\kappa - 1)/\kappa, \qquad \text{with } y_t = -\frac{1}{1 - \frac{1}{t}}. \tag{A5}$$

To calculate confidence intervals of the GEV parameter or the return levels standard errors of these values are used. Calculating the confidence interval, for example, the shape parameter helps to decide, if the GEV distribution could be replaced by a more specified distribution such as the Gumbel, Frechet or Weibull distributions. As an example the standard error σ_{x_p} of a return level x_p is calculated using the delta method

$$\sigma_{x_p}^2 = \left(\frac{\delta}{\delta\zeta}x_p(\zeta, \beta, \kappa)\right)^2 \sigma_\zeta^2 + \left(\frac{\delta}{\delta\beta}x_p(\zeta, \beta, \kappa)\right)^2 \sigma_\beta^2$$
$$+ \left(\frac{\delta}{\delta\kappa}x_p(\zeta, \beta, \kappa)\right)^2 \sigma_\kappa^2, \tag{A6}$$

where σ_ζ is the standard error of the location parameter, σ_β the standard error of the scale parameter, and σ_κ standard error of the shape parameter.

References

Barriopedro, D., Garcia-Herrera, R., Lupo, A. R. and Hernandez, E. 2006. A climatology of Northern Hemisphere blocking. *J. Clim.* **19**, 1042–1063.

Black, E., Blackburn, M., Harison, G., Hoskins, B. J. and Methven, J. 2004. Factors contributing to the summer 2003 European heatwave. *Weather* **59**, 217–223.

Blender, R., Fraedrich, K. and Lunkeit, F. 1997. Identification of cyclone-track regimes in the North Atlantic. *Quart. J. Roy. Meteor. Soc.* **123**, 727–741.

Charney, J. G. and DeVore, J. G. 1979. Multiple flow equilibria in the atmosphere and blocking. *J. Atmos. Sci.* **36**, 1205–1216.

Croci-Maspoli, M., Schwierz, C. and Davies, H. C. 2007. A multifaceted climatology of atmospheric blocking and its recent linear trend. *J. Clim.* **20**, 633–649.

Egger, J. 1978. Dynamics of blocking high. *J. Atmos. Sci.* **35**, 1788–1801.

Fraedrich, K., Bantzer, C. and Burkhardt, U. 1993. Winter climate anomalies in Europe and their associated criculation at 500 hPa. *Clim. Dyn.* **8**, 161–175.

Frich, P., Alexandersson, H., Ashcroft, J., Dahlstroem, B., Demaree, G.R. and co-authors, 1996. North Atlantic climatological dataset (NACD Version 1) final report. Technical report, Danish Meteorological Institute, Scientific Report. 96-1.

Frich, P., Alexander, L. V., Della-Marta, P., Gleason, B., Haylock, M., and co-authors. 2002. Observed coherent changes in climatic extremes during the second half of the twentieth century. *Clim. Res.* **19**, 193–212.

Garcia-Herrera, R., Paredes, D., Trigo, R. M., Trigo, I. F., Hernandez, E., and co-authors. 2007. The outstanding 2004 – 2005 drought in the Iberian Peninsula: impacts and atmospheric circulation associated. *J. Hydrometeorol.* **8**, 483–498.

Hoskins, B. J. and Sardeshmukh, P. D. 1987. A diagnostic study of dynamics of the northern hemisphere winter of 1985-1986. *Quart. J. Roy. Meteor. Soc.* **113**, 759–778.

Hoskins, B. J., McIntyre, M. E. and Robertson, A. W. 1985. On the use and significance of isentropic potential vorticity maps. *Quart. J. Roy. Meteor. Soc.* **111**, 877–946.

Lejenäs, H. and Økland, H. 1983. Characteristics of Nothern Hemisphere blocking as determined from a time series of observational data. *Tellus* **35A**, 350–362.

Nakamura, H. and Fukamachi, T. 2004. Evolution and dynamics of summertime blocking over the Far East and the associated surface Okhotsk high. *Quart J. Roy. Meteor. Soc.* **130**, 1213–1233.

Nakamura, H., Nakamura, M. and Anderson, J. L. 1997. The role of high- and low-frequency dynamics in blocking formation. *Mon. Wea. Rev.* **125**, 2074–2093.

O'Kane, T. J. and Frederiksen, J. S. 2008. A comparison of statistical dynamical and ensemble prediction methods during blocking. *J. Atmos. Sci.* **65**, 426–447.

Pelly, J. L. and Hoskins, B. J. 2003. A new perspective on blocking. *J. Atmos. Sci.* **60**, 743–755.

Rex, D. F. 1950. Blocking action in the middle troposphere and its effect upon regional climate. I. An aerological study of blocking action. *Tellus* **2**, 196–211.

Sausen, R., König, W. and Sielmann, F. 1995. Analysis of blocking events from observations and ECHAM model simulations. *Tellus* **47A**, 421–438.

Scherrer, S. C., Croci-Maspoli, M., Schwierz, C. and Appenzeller, C. 2006. Two-dimensional indices of atmospheric blocking and their statistical relationship with winter climate patterns in the Euro-Atlantic region. *Int. J. Climatol.* **26**, 233–249.

Schwierz, C., Croci-Maspoli, M. and Davies, H. C. 2004. Perspicacious indicators of atmospheric blocking. *Geophys. Res. Lett.* **31**, L06125. doi:10.1029/2003GL019341

Shabbar, A., Huang, J. P. and Higuchi, K. 2001. The relationship between the wintertime North Atlantic Oscillation and blocking episodes in the North Atlantic. *Int. J. Clim.* **21**, 95–108.

Sillmann, J. and Croci-Maspoli, M. 2009. Present and future atmospheric blocking and its impact on European mean and extreme climate. *Geophys. Res. Lett.* **36**. L10702. doi:10.1029/2009GL038259

Sinclair, M. R. 1996. A climatology of anticyclones and blocking for the southern hemisphere. *Mon. Wea. Rev.* **124**, 245–263.

Takaya, K. and Nakamura, H. 2005a. Geographical dependence of upper-level blocking formation associated with intraseasonal amplification of the Siberian high. *J. Atmos. Sci.* **62**, 4441–4449.

Takaya, K. and Nakamura, H. 2005b. Mechanisms of intraseasonal amplification of the cold Siberian high. *J. Atmos. Sci.* **62**, 4423–4440.

Thompson, D. W. J., Wallace, J. M. and Hegerl, G. 2000. Annular modes in the extratropical circulation. Part II: Trends. *J. Clim.* **13**, 1018–1036.

Tibaldi, S. and Molteni, F. 1990. On the operational predictability of blocking. *Tellus* **42A**, 343–365.

Trigo, R. M., Trigo, I. F., DaCamara, C. C. and Osborn, T. J. 2004. Climate impact of the European winter blocking episodes from the NCEP/NCAR reanalyses. *Clim. Dyn.* **23**, 17–28.

Trigo, R. M., Garcia-Herrera, R., Diaz, J., Trigo, I. F. and Valente, M. A. 2005. How exceptional was the early August 2003 heatwave in France? *Geophys. Res. Lett.* **32**, L10701. doi:10.1029/2005GL022410

Tyrlis, E. and Hoskins, B. J. 2008a. Aspects of Northern Hemi-sphere atmospheric blocking climatology. *J. Atmos. Sci.* **65**, 1638–1652.

Tyrlis, E. and Hoskins, B. J. 2008b. The morphology of Northern Hemi-sphere blocking. *J. Atmos. Sci.* **65**, 1653–1665.

Wilks, D. S. 2006. *Statistical Methods in the Atmospheric Sciences*. Acadamic Press.

Woollings, T., Hoskins, B., Blackburn, M. and Berrisford, P. 2008. A new Rossby wave-breaking interpretation of the North Atlanitc Os-cillation. *J. Atmos. Sci.* **65**, 609–626.